

Review Article

The Computation of Radiation Transport Using Feautrier Variables I. Static Media

DIMITRI MIHALAS*

*Max-Planck-Institut für Physik und Astrophysik, Institut für Astrophysik,
Karl-Schwarzschild-Strasse 1, D-8046 Garching bei München,
Federal Republic of Germany*

Received March 28, 1984

A review is presented of methods for solving the radiation transport equation in terms of the symmetric and antisymmetric averages first introduced by Feautrier (*C.R. Acad. Sci. Paris* **258** (1964), 3189). These methods have enjoyed good success and have achieved considerable popularity in astrophysics. Both formulation and algorithms are discussed briefly, and basic references are provided in order to provide easy access to workers in other fields where these methods may prove applicable. © 1985 Academic Press, Inc.

I. INTRODUCTION

Radiation transport is of immense importance in astrophysics, because it not only plays a fundamental role in determining the structure and dynamics of astrophysical media, but also determines the emergent spectra which the astronomer must analyze in order to diagnose the physical state of objects he observes. It is therefore not surprising that astrophysicists have devoted a great deal of effort to solving the radiation transport problem. A diverse assortment of methods has been developed, and there is not unanimity of opinion as to which is best. Nevertheless one particular class of methods, based on Feautrier's idea [13-15] of using *symmetric* and *antisymmetric averages* of the radiation field along a ray, has gained prominence and popularity in astrophysics because it has led to a number of efficient, accurate, and robust algorithms. The purpose of this article is to provide workers in other areas of computational physics a concise introduction to this approach and to the literature it has spawned. We deal here only with static media; dynamical media and problems of line formation in moving media will be discussed in later articles.

Methods using Feautrier variables treat the transfer equation as a *differential*

* Alexander von Humboldt Stiftung Senior U.S. Scientist Awardee. Permanent address: High Altitude Observatory, National Center for Atmospheric Research, Boulder, Colorado.

equation (often in second-order form) subject to 2-point boundary conditions. An advantage of such an approach, as opposed to integral-equation formulations, is that it is very easy to incorporate new physics into the problem, e.g., complex scattering processes with partial redistribution in angle and frequency, velocity fields, relativistic effects, etc. Moreover these methods are naturally posed for dynamical problems and are easily adapted to radiation hydrodynamics codes. Of course they have disadvantages too. Thus the 2-point boundary-value nature of the technique implies it is "implicit" in space, requiring a recursive forward-backward sweep of the mesh. This requirement imposes little if any penalty in 1-dimensional problems, but makes the approach quite costly in two dimensions [9, 10, 36]. We therefore shall discuss only 1-dimensional media. Furthermore as the discretization scheme generally presupposes the radiation field is representable as a second-order polynomial on successive triads of mesh points, it is ill-suited to problems in which the photon mean free path varies radically from cell to cell, e.g., at material interfaces. It usually suffices to assume 1-material media in astrophysical problems, but even then special techniques must be employed at unresolved shocks or ionization fronts [33, 50]. For simplicity we shall henceforth assume all structures are resolved on the computational mesh; for problems with unavoidable unresolved interfaces only integral-equation formulations are generally rugged enough to survive, and the reader is advised to turn elsewhere.

In this article we focus on the mathematical structure, and on methodological and computational aspects of the problem; physical background can be found in [31, 40, 45]. Further, we shall discuss only direct solutions of the equations as these are easily vectorizable and are usually competitive in 1-dimensional problems. But we must note that for certain problems iterative solutions are indispensable, and although little experience has accumulated yet, a number of ingenious approaches are now being explored; these hold promise for the future.

II. PLANAR GEOMETRY

Consider first planar geometry. In astrophysics the paradigm is a stratified semi-infinite stellar atmosphere or a finite slab representing, say, a nebula.

A. *Second-Order Form of the Transfer Equation*

(i) Derivation. Let z measure distance in a direction \mathbf{k} perpendicular to the planar layers and let $\mu = \mathbf{n} \cdot \mathbf{k}$ be the angle cosine of the direction of photon propagation \mathbf{n} . Then for radiation moving in two antiparallel pencils around $\pm\mu$ we have the two transfer equations

$$\pm\mu(\partial I_{\mu\nu}/\partial z) = \chi_\nu(S_\nu - I_{\mu\nu}). \quad (2.1)$$

In Eq. (2.1), χ_ν is the total extinction coefficient or opacity (sum of "true absorption" plus "scattering") and S_ν is the total source function, which contains both thermal emission and scattering terms.

Define a mean-intensity-like variable by the symmetric average

$$j_{\mu\nu} \equiv \frac{1}{2}[I(+\mu, \nu) + I(-\mu, \nu)], \quad (0 \leq \mu \leq 1) \quad (2.2)$$

and a flux-like variable by the antisymmetric average

$$h_{\mu\nu} \equiv \frac{1}{2}[I(+\mu, \nu) - I(-\mu, \nu)], \quad (0 \leq \mu \leq 1). \quad (2.3)$$

Then adding the two equations (2.1) for $\pm\mu$ we obtain

$$\mu(\partial h_{\mu\nu}/\partial z) = \chi_\nu(j_{\mu\nu} - S_\nu), \quad (2.4)$$

and subtracting them we have

$$\mu(\partial j_{\mu\nu}/\partial z) = \chi_\nu h_{\mu\nu}. \quad (2.5)$$

Notice that these angle-dependent equations have a direct correspondence with the moment equations (2.34)–(2.36), and thus provide a natural framework for treating the interaction between matter and radiation in a physically satisfying way. Unlike the moment equations, these equations “close,” that is, they contain only $j_{\mu\nu}$ and $h_{\mu\nu}$ (because these two variables together manifestly specify $I_{\mu\nu}$ completely).

Using Eq. (2.5) to eliminate $h_{\mu\nu}$ from Eq. (2.4) we obtain the second-order form

$$\frac{\mu^2}{\chi_\nu} \frac{\partial}{\partial z} \left(\frac{1}{\chi_\nu} \frac{\partial j_{\mu\nu}}{\partial z} \right) = \mu^2 \frac{\partial^2 j_{\mu\nu}}{\partial \tau_\nu^2} = j_{\mu\nu} - S_\nu, \quad (0 \leq \mu \leq 1), \quad (2.6)$$

where the optical depth τ_ν , measured inward, is defined as

$$d\tau_\nu = -\chi_\nu dz. \quad (2.7)$$

Note that in writing Eq. (2.5) we have tacitly assumed that χ_ν and S_ν are isotropic, or at least are even functions of μ (e.g., the dipole phase function of Thomson or Rayleigh scattering). When this is not the case [43], an additional source term appears in Eq. (2.5) and we cannot combine Eqs. (2.4) and (2.5) into the second-order form of Eq. (2.6). We must then solve the coupled first-order equations using an algorithm similar to that described in Section III.B.

(ii) Boundary conditions. Equation (2.6) must be supplemented by boundary conditions at $\tau_\nu = 0$ and $\tau_\nu = \tau_{\max}$; these are of the general form $c_1 + c_2 j_{\mu\nu} + c_3 (\partial j_{\mu\nu}/\partial \tau_\nu) = 0$. For example, suppose an incoming intensity $I_{\mu\nu}^-$ is imposed at $\tau_\nu = 0$ and an outgoing intensity $I_{\mu\nu}^+$ at $\tau_\nu = \tau_{\max}$. Then using the identity

$$h_{\mu\nu} \equiv j_{\mu\nu} - I(-\mu, \nu) \equiv I(+\mu, \nu) - j_{\mu\nu}, \quad (2.8)$$

we have

$$\mu(\partial j_{\mu\nu}/\partial \tau_\nu)_0 = j_{\mu\nu}(0) - I_{\mu\nu}^- \quad (2.9)$$

and

$$\mu(\partial j_{\mu\nu}/\partial\tau_\nu)_{\tau_{\max}} = I_{\mu\nu}^+ - j_{\mu\nu}(\tau_{\max}). \quad (2.10)$$

Alternatively, deep within a semi-infinite medium we can impose the equilibrium diffusion approximation and take

$$I_{\mu\nu}(\tau_{\max}) \approx B_\nu(\tau_{\max}) + \mu(\partial B_\nu/\partial\tau_\nu)_{\tau_{\max}}, \quad (2.11)$$

whence we have $j_{\mu\nu}(\tau_{\max}) = B_\nu$ and $h_{\mu\nu}(\tau_{\max}) = \mu(\partial B_\nu/\partial\tau_\nu)_{\tau_{\max}}$. We can then write a boundary condition

$$(\partial j_{\mu\nu}/\partial\tau_\nu)_{\tau_{\max}} = (\partial B_\nu/\partial\tau_\nu)_{\tau_{\max}} = -(1/\chi_\nu)(\partial B_\nu/\partial T)(dT/dz)_{\tau_{\max}}. \quad (2.12)$$

If the medium is static and in a steady state then it is in radiative equilibrium, hence we can specify a constant imposed radiation flux at the lower boundary. Exploiting the diffusion approximation we obtain

$$H = \int_0^\infty dv \int_0^1 d\mu \mu h_{\mu\nu} = -(dT/dz) \int_0^\infty dv \chi_\nu^{-1} (\partial B_\nu/\partial T) \int_0^1 d\mu \mu^2, \quad (2.13)$$

so that we can rewrite Eq. (2.12) as

$$\left(\frac{\partial j_{\mu\nu}}{\partial\tau_\nu}\right)_{\tau_{\max}} = \frac{3H}{\chi_\nu} \left(\frac{\partial B_\nu}{\partial\tau}\right) \Big/ \int_0^\infty \frac{1}{\chi_\nu} \frac{\partial B_\nu}{\partial\tau} dv = 3H \left(\frac{\chi_R}{\chi_\nu}\right) \frac{(\partial B_\nu/\partial\tau)}{(dB/dT)}, \quad (2.14)$$

where χ_R is the usual Rosseland mean opacity and $B = \sigma T^4/\pi$.

(iii) Discretization. Equations (2.6), (2.9), and a choice of (2.10), (2.12), or (2.14) specify the radiation field completely (for a given run of material properties in the medium). To solve them we discretize all variables, choosing a mesh of angle-points $\{\mu_m\}$ ($m = 1, \dots, M$) and frequency-points $\{\nu_n\}$ ($n = 1, \dots, N$) spanning the ranges $0 \leq \mu \leq 1$ and $0 \leq \nu \leq \infty$. The medium is divided into discrete cells. The variables $j_{\mu\nu}$ may be located either at the cell surface $\{z_d\}$ ($d = 1, \dots, D$) or at the center of a set of mass cells $\{\Delta m_{d+1/2}\}$ ($d = 1, \dots, D$). The former choice has usually been adopted in static or steady-flow stellar atmospheres and quasi-static stellar evolution work. The

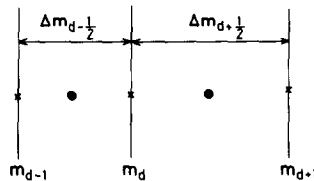


FIG. 1. Variables located at cell centers (●): ρ , T , p , e , $j_{\mu\nu}$, E_ν , P_ν ; variables located at cell boundaries (x): z (or r), u , $h_{\mu\nu}$, F_ν .

latter is more natural for dynamical applications on a Lagrangean or adaptive mesh using a staggered-mesh scheme such as sketched in Fig. 1; to be consistent with later topics of discussion we adopt this scheme here.

Variables located at cell centers are given half-integral indices, e.g., $j_{d+1/2,mn} \equiv j(m_{d+1/2}, \mu_m, \nu_n)$; those at cell surfaces are given integral indices, e.g., h_{dmn} . Derivatives are replaced with finite differences and angle-frequency integrals in the source terms (see Sect. IIC) are replaced with quadrature sums, e.g.,

$$\int_0^{\infty} y(\nu) d\nu \rightarrow \sum_{n=1}^N a_n y(\nu_n) \quad (2.15)$$

and

$$\int_0^1 y(\mu) d\mu \rightarrow \sum_{m=1}^M b_m y(\mu_m), \quad (2.16)$$

where the a 's and b 's are appropriate quadrature weights. It is convenient to concatenate all combinations of angles and frequencies into a single set with index $k = 1, \dots, K$ (e.g., $(\mu_k, \nu_k) = (\mu_m, \nu_n)$ with $k = m + (n - 1)M$).

We thus replace Eq. (2.6) with a difference representation such as

$$\begin{aligned} & \frac{\mu_k^2}{\Delta\tau_{d+1/2,k}} \left[\frac{1}{\Delta\tau_{d+1,k}} j_{d+3/2,k} - \left(\frac{1}{\Delta\tau_{dk}} + \frac{1}{\Delta\tau_{d+1,k}} \right) j_{d+1/2,k} + \frac{1}{\Delta\tau_{dk}} j_{d-1/2,k} \right] \\ & = j_{d+1/2,k} - S_{d+1/2,k}, \quad (k = 1, \dots, K), (d = 2, \dots, D - 1). \end{aligned} \quad (2.17)$$

Here

$$\Delta\tau_{dk} \equiv \frac{1}{2}(\omega_{d-1/2,k} \Delta m_{d-1/2} + \omega_{d+1/2,k} \Delta m_{d+1/2}) \quad (2.18)$$

and

$$\Delta\tau_{d+1/2,k} \equiv \frac{1}{2}(\Delta\tau_{dk} + \Delta\tau_{d+1,k}), \quad (2.19)$$

where $\omega_\nu \equiv \chi_\nu/\rho$. The source function has the general form

$$S_{d+1/2,k} = \alpha_{d+1/2,k} \sum_{k'=1}^K w_{k'} j_{d+1/2,k'} + \beta_{d+1/2,k}. \quad (2.20)$$

Equation (2.17) is second-order accurate. Auer [4] has developed a fourth-order accurate Hermite representation of Eq. (2.6), and some authors [24, 38] have used spline collocation techniques; in both cases the system retains a tridiagonal structure as in Eq. (2.17) and the algorithms described below are unaffected.

When $j_{\mu\nu}$ is chosen to lie on cell surfaces, second-order accurate discrete boundary conditions are easily derived by Taylor series expansion [2], and with Hermite

formulae one obtains third-order accuracy [4]. For a staggered mesh one proceeds as follows: At the upper boundary Eq. (2.4) gives

$$h_{2k} = \mu_k(j_{5/2k} - j_{3/2k})/\Delta\tau_{2k} \quad (2.21)$$

and Eq. (2.4) gives

$$h_{2k} = h_{1k} + (\Delta\tau_{3/2k}/\mu_k)(j_{3/2k} - S_{3/2k}), \quad (2.22)$$

where $\Delta\tau_{3/2k} \equiv \omega_{3/2k} \Delta m_{3/2}$. Applying Eq. (2.9) from the surface of the uppermost cell to its center we have

$$h_{1k} = j_{1k} - I^- = \mu_k(j_{3/2k} - j_{1k})/\frac{1}{2} \Delta\tau_{3/2k}, \quad (2.23)$$

whence we find

$$h_{1k} = (j_{3/2k} - I^-)/(1 + \frac{1}{2} \Delta\tau_{3/2k}/\mu_k). \quad (2.24)$$

Combining Eqs. (2.21), (2.22), and (2.24) we obtain the desired boundary condition

$$\begin{aligned} \mu_k(j_{5/2k} - j_{3/2k})/\Delta\tau_{2k} &= [(j_{3/2k} - I^-)/(1 + \frac{1}{2} \Delta\tau_{3/2k}/\mu_k)] \\ &+ (\Delta\tau_{3/2k}/\mu_k)(j_{3/2k} - S_{3/2k}). \end{aligned} \quad (2.25)$$

At the lower boundary one discretizes Eq. (2.10), (2.12), or (2.14); in particular, Eq. (2.14) implies

$$\frac{(j_{D+1/2,k} - j_{D-1/2,k})}{\Delta\tau_{Dk}} = \frac{3H}{\omega_{D+1/2,k}} \left(\frac{\partial B_k}{\partial T} \right)_{D+1/2} \bigg/ \sum_{n=1}^N \frac{a_n}{\omega_{D+1/2,n}} \left(\frac{\partial B_n}{\partial T} \right)_{D+1/2}. \quad (2.26)$$

Equation (2.26) is only of first-order accuracy, but that is usually sufficient in the equilibrium diffusion regime.

(iv) Remarks. Equations (2.17), (2.25), and (2.26) comprise a block tridiagonal system of order DK for the unknowns $J_{d+1/2,k}$. To solve them we must clearly perform a forward-backward recursive sweep to match the 2-point boundary conditions. Thus, as mentioned in Section I, the equations are "implicit" in space, which is unfavorable in multidimensional problems. On the other hand, the symmetric and antisymmetric averages $j_{\mu\nu}$ and $h_{\mu\nu}$ naturally and automatically locate radiation tensors of even rank at cell centers and tensors of odd rank at cell boundaries, just where these quantities are needed. More important, because the cancellation between $I(+\mu)$ and $I(-\mu)$ is done *analytically* in $h_{\mu\nu}$ and $h_{\mu\nu}$ is retained as a variable (more precisely, is recoverable at will from Eq. (2.5)), one can compute accurate radiation fluxes without suffering the severe numerical cancellation at large optical depths that results if he were to calculate $I(+\mu)$ and $I(-\mu)$ separately and then subtract. In addition, the Feautrier system is automatically consistent with second-order diffusion (see Sects. 83, 97 of [40]). Both of these features are obviously

of prime importance in obtaining accurate energy balance in the radiating fluid and give Feautrier methods significant physical advantages over many other methods.

B. The Formal Solution

The difficulty of solving the transfer equation depends on what is assumed to be known about the source function S_ν and its coupling to the radiation field and/or material properties. The simplest problem of all is a *formal solution*, in which we are to calculate the radiation field at all depths, angles, and frequencies when the source function is *given*. A formal solution is required in order to know the radiation field emergent from the medium; it is also almost always needed in iterative procedures used to solve more complex problems.

Represent the depth variation of $j(\mu_k, \nu_k)$ by the column vector

$$\mathbf{j}_k \equiv (j_{3/2k}, j_{5/2k}, \dots, j_{D+1/2,k}) \quad (2.27)$$

and the (known) depth variation of $S(\nu_k)$ by S_k . Then the transfer equation and boundary conditions are of the form

$$\mathbf{T}_k \mathbf{j}_k = S_k, \quad (2.28)$$

where \mathbf{T}_k is a $(D \times D)$ tridiagonal matrix. The system is solved by the standard tridiagonal Gaussian elimination scheme. The computational work scales as $cDK = cDMN$, which is irreducible because we seek DK values of $j_{\mu\nu}$. On vector machines one can vectorize the recursive depth elimination over angle frequency and solve K systems in parallel with a corresponding large increase in speed [20].

C. Scattering Problems

More generally, we must face up to the integrodifferential nature of the system implied by source terms of the general form of Eq. (2.20). The bandwidth of the integrals in the angle-frequency domain is determined by the physical processes described by the scattering kernel (see Chaps. 2, 7, 12, and 13 of [31]). For example: (a) For isotropic or angle-dependent coherent scattering all angles are coupled at each frequency separately. (b) For line-formation problems with complete, or angle-averaged partial frequency redistribution the source function contains only angular moments of the radiation field. Thus angles are eliminated but all frequencies within the line are coupled. (c) More generally, in multilevel statistical equilibrium calculations all frequencies within the transition array are coupled. (d) Yet more generally, for line-formation problems with angle-dependent partial redistribution in static media, or even complete redistribution in moving media, all angles and frequencies are coupled explicitly and inextricably, and a meaningful splitting of these two dimensions is no longer possible. The same remark holds a fortiori for radiation transport in relativistic flows where the coupling among the components of the photon 4-momentum in the tangent spaces attached to world lines is essentially complete [32, 42]. Similar couplings occur in other physical arenas, e.g., neutron

transport, and is often treated successfully by iterative schemes. For a variety of reasons (see, e.g., Chaps. 6 and 11 of [31]) such schemes generally fail in radiation transport applications, and hard experience has shown that it is best, and usually necessary, to treat *essential* couplings directly; that is the route taken here.

(i) The Feautrier algorithm. In the *Feautrier algorithm* [13] one defines vectors

$$\mathbf{j}_{d+1/2} = (j_{d+1/2,1}, j_{d+1/2,2}, \dots, j_{d+1/2,K}), \quad (d = 1, \dots, D), \quad (2.29)$$

containing the angle-frequency (either or both) dependence of the radiation field deemed necessary to describe S at a single depthpoint. The discretized transport equation is then of the form

$$-\mathbf{A}_{d+1/2}\mathbf{j}_{d-1/2} + \mathbf{B}_{d+1/2}\mathbf{j}_{d+1/2} - \mathbf{C}_{d+1/2}\mathbf{j}_{d+3/2} = \mathbf{L}_{d+1/2}, \quad (2.30)$$

where \mathbf{A} , \mathbf{B} , and \mathbf{C} are $(K \times K)$ matrices and \mathbf{L} is a vector of length K containing the thermal source terms from Eq. (2.20). If the second-order scheme of Eq. (2.17) is used, \mathbf{B} is full but \mathbf{A} and \mathbf{C} are diagonal. If Hermite or spline collocation formulae are used, \mathbf{A} and \mathbf{C} become full as well; the reduction in number of depthpoints afforded by these higher-order schemes may therefore be more than offset by the increased computation required in Eqs. (2.31)–(2.33). The upper and lower boundary conditions imply $\mathbf{A}_{3/2} \equiv 0$ and $\mathbf{C}_{D+1/2} \equiv 0$. The system is solved by computing

$$\mathbf{D}_{d+1/2} \equiv (\mathbf{B}_{d+1/2} - \mathbf{A}_{d+1/2}\mathbf{D}_{d-1/2})^{-1}\mathbf{C}_{d+1/2} \quad (2.31)$$

and

$$\mathbf{v}_{d+1/2} \equiv (\mathbf{B}_{d+1/2} - \mathbf{A}_{d+1/2}\mathbf{D}_{d-1/2})^{-1}(\mathbf{L}_{d+1/2} + \mathbf{A}_{d+1/2}\mathbf{v}_{d-1/2}) \quad (2.32)$$

for $d = 1, \dots, D$. The LU decomposition of $(\mathbf{B} - \mathbf{AD})$ is vectorizeable [21] as is the generation of the multiple right-hand sides in Eqs. (2.31) and (2.32) [22]. When \mathbf{C} is sparse, it may be faster on scalar machines to actually compute the inverse $(\mathbf{B} - \mathbf{AD})^{-1}$ and then take advantage of the structure of \mathbf{C} in computing \mathbf{D} . Because $\mathbf{C}_{D+1/2} = 0$, $\mathbf{D}_{D+1/2} = 0$, hence $\mathbf{j}_{D+1/2} \equiv \mathbf{v}_{D+1/2}$. The radiation field is then constructed by the back-substitution

$$\mathbf{j}_{d+1/2} = \mathbf{D}_{d+1/2}\mathbf{j}_{d+3/2} + \mathbf{v}_{d+1/2}, \quad (d = D - 1, \dots, 1). \quad (2.33)$$

The total computational effort scales as $cDK^3 = cDM^3N^3$. Notice that the Feautrier algorithm is cheap for coherent scattering ($N = 1$) but rapidly becomes costly as the frequency bandwidth of the source term increases.

(ii) Moment equations and variable Eddington factors. The unfavorable scaling of the computing effort in the basic Feautrier method as $K^3 \propto M^3N^3$ shows that it is imperative to eliminate any inessential information contained in the solution vector. In particular, unless the angular coupling in S_ν is absolutely indispensable (as in case

(d) discussed at the beginning of Sect. II.C], we should replace Eqs. (2.6), (2.9), and say, (2.14) by the angle-integrated moment equations

$$\partial^2(f_\nu J_\nu)/\partial\tau_\nu^2 = J_\nu - S_\nu, \quad (2.34)$$

$$[\partial(f_\nu J_\nu)/\partial\tau_\nu]_0 = H_\nu(0), \quad (2.35)$$

and

$$[\partial(f_\nu J_\nu)/\partial\tau_\nu]_{\tau_{\max}} = H[(\chi_R/\chi_\nu)(\partial B_\nu/\partial T)/(dB/dT)]_{\tau_{\max}}, \quad (2.36)$$

where $J_\nu \equiv \int_0^1 j_{\mu\nu} d\mu$ is the mean intensity, $H_\nu \equiv \int_0^1 h_{\mu\nu} \mu d\mu$ is the (Eddington) flux, and $H \equiv \int_0 H_\nu d\nu = \text{constant}$.

In Eqs. (2.34)–(2.36), f_ν denotes the *variable Eddington factor* [16]

$$f_\nu \equiv \frac{K_\nu}{J_\nu} = \frac{\int_0^1 j_{\mu\nu} \mu^2 d\mu}{\int_0^1 j_{\mu\nu} d\mu} = \frac{P_\nu}{E_\nu}; \quad (2.37)$$

here E_ν and P_ν are the monochromatic radiation energy density and pressure. This factor provides *closure* of the system of moments. If f_ν and the additional form factor $g_\nu \equiv H_\nu(0)/J_\nu(0)$ are regarded as known, then discretized versions of Eqs. (2.34)–(2.36) are of the same form as Eq. (2.30) and can be solved by the same algorithm.

We thus proceed by iteration [6]: (1) Given f_ν 's and g_ν (good initial guesses are $f_\nu \equiv \frac{1}{3}$ and $g_\nu \equiv \frac{1}{2}$, obtained by assuming $j_{\mu\nu}$ is isotropic and $I^- = 0$), we solve the frequency-coupled moment equations (2.34)–(2.36). In doing so we obtain correct global thermalization of J_ν (see Chaps. 6 and 11 of [31]). (2) Using the resulting J_ν 's we can evaluate S_ν , and then perform a formal solution to construct the full angle-frequency dependent distribution function $j_{\mu\nu}$. We can then update the Eddington factors from

$$f_{d+1/2,n} = \sum_{m=1}^M b_m \mu_m^2 j_{d+1/2,mn} \left/ \sum_{m=1}^M b_m j_{d+1/2,mn} \right. \quad (2.38)$$

Likewise we can use Eq. (2.23) to evaluate j_{1mn} and h_{1mn} , hence the surface factors f_{1n} and g_n . With new Eddington factors we return to step (1) and iterate to convergence.

For I iterations the computational effort scales as $I(cDMN + c'DN^3) \ll c''DM^3N^3$ even for modest M provided I is not large. Extensive experience has shown this procedure to be strongly convergent; typically only 3 or 4 iterations are required to determine the f_ν 's with good accuracy [6], hence large savings are realized even for $M = 3$ or 4. The reason this splitting works so well is that the radiation field is, in fact, essentially isotropic for $\tau_\nu > 1$, hence the iteration is needed only in an optically thin boundary layer.

(ii) The Rybicki algorithm. In certain problems the frequency coupling in the source function is all contained in a single quantity which is not itself explicitly

frequency dependent. For example, in line-formation problems with complete redistribution the scattering term contains only $\bar{J} \equiv \int \phi_\nu J_\nu d\nu$, where ϕ_ν is the line profile (see Chap. 11 of [31]); a similar situation arises if we demand energy balance (see Sect. II.D). In such cases the frequency information retained by the Feautrier algorithm is redundant and, as shown by Rybicki [46], a much more efficient algorithm results from interchanging the inner and outer structure of the system.

Thus assume the source function has the form $S_\nu = \alpha_\nu \bar{J} + \beta_\nu$, where \bar{J} is some integral over J_ν (or double integral over $j_{\mu\nu}$). Let

$$\bar{\mathbf{J}} \equiv (\bar{J}_{3/2}, \bar{J}_{5/2}, \dots, \bar{J}_{D+1/2}) \quad (2.39)$$

represent the run of \bar{J} with depth. Then for each angle-frequency point the transfer equation (2.17) plus boundary conditions has the form

$$\mathbf{T}_k \mathbf{j}_k + \mathbf{U}_k \bar{\mathbf{J}} = \mathbf{K}_k, \quad (k = 1, \dots, K), \quad (2.40)$$

where \mathbf{T}_k is a $(D \times D)$ tridiagonal matrix representing the differential operator, \mathbf{U}_k is a diagonal or tridiagonal $(D \times D)$ matrix (for second-order or Hermite schemes, respectively) containing the depth variation of the coupling coefficient $\alpha_{d+1/2,k}$ of the scattering term, and \mathbf{K}_k is a vector containing the depth variation of the thermal source term $\beta_{d+1/2,k}$. In addition there are D equations defining $\bar{\mathbf{J}}$, namely

$$\bar{J}_{d+1/2} = \sum_{k=1}^K w_{d+1/2,k} j_{d+1/2,k}, \quad (d = 1, \dots, D), \quad (2.41)$$

where the weights account for profile functions. Equations (2.41) are equivalent to

$$\bar{\mathbf{J}} = \sum_{k=1}^K \mathbf{V}_k \mathbf{j}_k, \quad (2.42)$$

where the \mathbf{V}_k 's are diagonal. For each k we solve Eq. (2.40) to find \mathbf{A}_k and \mathbf{B}_k in

$$\mathbf{j}_k = \mathbf{A}_k - \mathbf{B}_k \bar{\mathbf{J}} = \mathbf{T}_k^{-1} \mathbf{K}_k - (\mathbf{T}_k^{-1} \mathbf{U}_k) \bar{\mathbf{J}}. \quad (2.43)$$

Substituting Eq. (2.43) into Eq. (2.42) for all k we develop the final system $\mathbf{C} \bar{\mathbf{J}} = \mathbf{D}$, where \mathbf{C} is full. Solving this system we obtain $\bar{\mathbf{J}}$, hence the run of S with depth. The radiation field can then be recovered by a formal solution (which is cheaper than evaluating Eq. (2.43)).

The calculation of each \mathbf{B}_k requires $O(D^2)$ operations, as does the summation of $\mathbf{V}_k \mathbf{B}_k$ into \mathbf{C} . Hence the total computing effort scales as $cD^2K + c'D^3 = cD^2MK + c'D^3$; in practice the first term usually dominates. Therefore the Rybicki scheme has an enormous advantage over the Feautrier scheme in problems with large numbers of angles and/or frequencies. On the other hand Feautrier's scheme can handle the most general case of partial redistribution (whereas Rybicki's method cannot), and is better suited to problems in which the radiative transfer is coupled to a large number of additional constraint equations, as we now show.

D. The Model Atmosphere Problem

(i) Momentum and energy balance. Pedagogical cases aside, radiation transport problems rarely arise in isolation, but in reality are coupled to other physical constraints such as momentum and energy balance. A good example is provided by the *model atmosphere problem* in which a static, stratified, semi-infinite medium radiates into vacuum. Because the medium is static, it is in radiative and hydrostatic equilibrium, hence

$$\int_0^{\infty} (4\pi\eta_v - c\chi_v E_v) dv = 4\pi \int_0^{\infty} \chi_v (S_v - J_v) dv = 0 \quad (2.44)$$

and

$$\frac{d}{dm} (p + P) = g \quad (2.45a)$$

or

$$(dp/dm) = g - (4\pi/c) \int_0^{\infty} \omega_v H_v dv. \quad (2.45b)$$

Here $p = NkT$ is the gas pressure (N is the total particle density); P is the total radiation pressure

$$P = \int_0^{\infty} P_v dv = \int_0^{\infty} f_v E_v dv = (4\pi/c) \int_0^{\infty} f_v J_v dv; \quad (2.46)$$

m is the column-mass measured inward

$$dm = -\rho dz; \quad (2.47)$$

g is the (constant) surface gravity; and η_v is the emissivity of the material, including both thermal and scattering terms. In discrete form we have

$$\sum_{n=1}^N a_n (\eta_{d+1/2,n} - \chi_{d+1/2,n} J_{d+1/2,n}) = 0, \quad (d = 1, \dots, D), \quad (2.48)$$

and

$$\begin{aligned} k(N_{d+1/2} T_{d+1/2} - N_{d-1/2} T_{d-1/2}) + (4\pi/c) \sum_{n=1}^N a_n (f_{d+1/2,n} J_{d+1/2,n} - f_{d-1/2,n} J_{d-1/2,n}) \\ = g \Delta m_d, \quad (d = 1, \dots, D), \end{aligned} \quad (2.49)$$

where $\Delta m_d \equiv \frac{1}{2}(\Delta m_{d-1/2} + \Delta m_{d+1/2})$. We obtain a boundary condition for $d = 1$ from Eq. (2.45b) by assuming the medium (if any) above m_1 is transparent so that H_ν is constant; then

$$N_{3/2} k T_{3/2} = m_1 g - (4\pi/c) \sum_{n=1}^N a_n \omega_{3/2n} h_n J_{3/2n}, \quad (2.50)$$

where h_ν is a form factor, obtained from a formal solution, relating $H_\nu(0)$ to J_ν at $d = \frac{3}{2}$.

Equations (2.44) and (2.45) are to be solved simultaneously with the transport equations, e.g., Eqs. (2.34)–(2.36). To complete the system we impose conditions of particle and charge conservation, and specify an algorithm for determining individual bound and free state occupation numbers as a function of N , T , and (in general) the radiation field. We then have a highly nonlinear system which must be solved iteratively.

(ii) LTE atmospheres by Feautrier algorithm. Suppose first that the material is in *local thermodynamic equilibrium* (LTE). One then assumes that material occupation numbers are determined solely by the equations of equilibrium statistical mechanics given *local* values of T and N . The radiation field, in contrast, is allowed to depart from its equilibrium distribution function $B_\nu(T)$ and to respond to spatial gradients and boundary effects. Explicit coupling of level populations to the radiation field is simply ignored, so this approximation can be expected to be correct only in the limit of high densities when collisional rates vastly exceed radiative rates [49; 31, Chap. 5].

Given the assumption of LTE, our problem is to determine the solution vectors

$$\Psi_{d+1/2} \equiv (J_{d+1/2,1}, \dots, J_{d+1/2,N}, T_{d+1/2}, N_{d+1/2}), \quad (d = 1, \dots, D), \quad (2.51)$$

from N discretized radiation moment equations (2.34)–(2.36) and the constraint equations (2.48)–(2.50), which collectively are of the form

$$\mathbf{f}_{d+1/2}(\Psi) = \mathbf{f}_{d+1/2}(\Psi_{d-1/2}, \Psi_{d+1/2}, \Psi_{d+3/2}) = 0. \quad (2.52)$$

To solve nonlinear system (2.52) we use the generalized Newton–Raphson technique (sometimes called “complete linearization” in astrophysics), so that given a trial solution Ψ^0 we calculate the correction $\delta\Psi$ that satisfies

$$\sum_j (\partial \mathbf{f}_{d+1/2} / \partial \psi_j) \delta \psi_j = -\mathbf{f}_{d+1/2}(\Psi^0), \quad (d = 1, \dots, D), \quad (2.53)$$

where j runs over all variables. Essentially all of the derivatives in Eq. (2.53) can be worked out analytically [5, 35]. The resulting system is block tridiagonal,

$$-\mathbf{A}_{d+1/2} \delta \Psi_{d-1/2} + \mathbf{B}_{d+1/2} \delta \Psi_{d+1/2} - \mathbf{C}_{d+1/2} \delta \Psi_{d+3/2} = \mathbf{E}_{d+1/2}, \quad (2.54)$$

and can be solved by the Feautrier algorithm. After each Newton–Raphson correction the variable Eddington factors needed in Eqs. (2.34)–(2.36) are updated in a formal solution using the revised model. A consequence of this procedure is loss of quadratic convergence, a sacrifice that must be made because direct inclusion of angle-dependent information escalates the computational effort prohibitively. In any event the critical bottleneck is to remain within the domain of convergence of the linearization procedure; details and special techniques are discussed in [35].

The computational effort of this approach scales as $cD(N+2)^3$, which is unfavorable because for physical reasons one often desires to use a large number of frequencies (e.g., to treat spectral line blanketing). Two approaches can be suggested to reduce the computational burden: (1) One can suppress the frequency dimension by integrating the transfer equation over frequency, introducing frequency-averaged *mean opacities* [12, 28]. Four means are required: the usual Planck and Rosseland means χ_P and χ_R , and energy- and flux-weighted means,

$$\chi_E \equiv \int_0^\infty \chi_\nu E_\nu dv/E \quad (2.55a)$$

and

$$\chi_F \equiv \int_0^\infty \chi_\nu F_\nu dv/F. \quad (2.55b)$$

The same means enter the radiative and hydrostatic equilibrium constraints. The computational strategy is to solve the frequency-integrated moment equations, regarding the *spectral profile* functions E_ν/E and F_ν/F as given (much in the same spirit as variable Eddington factors), and approach strongly reminiscent of the *multifrequency/grey* technique of the VERA code [16]. In order to linearize the equations one may write $\chi_E = k_E \chi_P(N, T)$ and $\chi_F = k_F \chi_R(N, T)$, and keep the factors k_E and k_F at each depth fixed under linearization. The result is a block tridiagonal system with only three depth-dependent variables— N , T , and J (or E)—which is cheap to solve. Each linearization step is followed by a full formal solution to provide updated variable Eddington factors and spectral profiles. Of course because less of the coupling is handled directly, this method converges more slowly than Eqs. (2.53) and (2.54); the cheapness of each iteration may offset their greater number, and often

with enormous opacity variations the method may simply fail, we must then revert to a calculation that handles the frequency coupling explicitly. (2) Alternatively one can apply formal *splittings* to the matrices in Eq. (2.54), and solve the frequency-dependent system by astute iterative techniques instead of by brute force. A good example of such a procedure is given in [8]; this approach does not seem to have been widely applied in astrophysics as yet.

(iii) LTE atmospheres by Rybicki algorithm. Another way of computing LTE model atmospheres economically is to use the Rybicki algorithm. Because it is

assumed that material properties depend only on N and T , the linearized transport equation at each frequency can be written

$$\mathbf{T}_k \delta \mathbf{J}_k + \mathbf{U}_k \delta \mathbf{N} + \mathbf{V}_k \delta \mathbf{T} = \mathbf{K}_k, \quad (2.56)$$

where $\delta \mathbf{J}_k$, $\delta \mathbf{N}$, and $\delta \mathbf{T}$ represent the depth variations of each of the indicated quantities and \mathbf{T}_k , \mathbf{U}_k , and \mathbf{V}_k are all tridiagonal. These systems can be solved (vectorizing over multiple right-hand sides) for expressions of the form

$$\delta \mathbf{J}_k = \mathbf{Q}_k \delta \mathbf{N} + \mathbf{R}_k \delta \mathbf{T} + \mathbf{S}_k, \quad (k = 1, \dots, K). \quad (2.57)$$

Equations (2.57) are substituted into the linearized constraints of hydrostatic and radiative equilibrium, which are of the forms

$$\sum_{k=1}^K \mathbf{W}_k \delta \mathbf{J}_k + \mathbf{A} \delta \mathbf{N} + \mathbf{B} \delta \mathbf{T} = \mathbf{Y} \quad (2.58)$$

and

$$\sum_{k=1}^K \mathbf{X}_k \delta \mathbf{J}_k + \mathbf{C} \delta \mathbf{N} + \mathbf{D} \delta \mathbf{T} = \mathbf{Z}, \quad (2.59)$$

to develop a final full system

$$\begin{pmatrix} \mathbf{E} & \mathbf{F} \\ \mathbf{G} & \mathbf{H} \end{pmatrix} \begin{pmatrix} \delta \mathbf{N} \\ \delta \mathbf{T} \end{pmatrix} = \begin{pmatrix} \mathbf{L} \\ \mathbf{M} \end{pmatrix} \quad (2.60)$$

which yields $\delta \mathbf{N}$ and $\delta \mathbf{T}$.

After revising the temperature-density structure of the medium, one performs a formal solution for all angles and frequencies to update Eddington factors. These are used in the updated Eqs. (2.56), and the whole process is iterated to convergence. The total computing effort scales as $I[cD^2N + c'(2D)^3]$, which is favorable in that it scales linearly with N . Thus the Rybicki method is to be preferred for LTE models having complicated frequency spectra. On the other hand, in imposing *two* constraints instead of one we are penalized by an eightfold increase in the effort needed to solve the final system (2.60).

In many applications this penalty can be evaded [17]. Notice that the hydrostatic equation is coupled to the radiation field through the radiation pressure gradient (or radiation force) term. When these terms are negligible compared to g (low-temperature media), the gas pressure p is simply a linear function of m and can be fixed once and for all. Even in high temperature media a good estimate of the radiation force is given by the diffusion theory result

$$dP/dm = (\chi_R/\rho c)(L/4\pi R^2) = (\chi_R/\rho c) \sigma T_{\text{eff}}^4 \quad (2.61)$$

where T_{eff} is the so-called effective temperature associated with the (constant) radiant flux or luminosity imposed at the lower boundary. These facts suggest that we rewrite Eqs. (2.56)–(2.60) in terms of δT and δp , and then merely drop terms in δp , solving only a $(D \times D)$ system for δT . The small changes in pressure structure produced by improved estimates of the radiation forces are then accounted for by an iterative update after the formal solution is performed to update Eddington factors.

(iv) Non-LTE atmosphere by the Feautrier algorithm. In astrophysical media densities are often low while radiation fields are large, particularly in the observable boundary layers of the objects under study. Here the ad hoc assumption of LTE breaks down and we must determine occupation numbers directly from steady state rate equations of the general form

$$-n_i \sum_{j \neq i} (R_{ij} + C_{ij}) + \sum_{j \neq i} n_j (R_{ji} + C_{ji}) = 0 \quad (2.62)$$

in which the R 's and C 's denote radiative and collisional rates, respectively, (see, e.g., Chaps. 5 of [31]). We then have a strongly interlocked system in which complex (and sometimes subtle) physical interactions occur (see, e.g., Chaps. 7, 11, and 12 of [31]), and therefore have little recourse but to account for all couplings in the most direct way possible.

Thus far the most successful approach [5, 7, 30, 34] has been to adjoin a set of L rate equations (one for each bound level plus one for total number conservation) and a charge conservation equation to the transport, radiative equilibrium, and hydrostatic equilibrium equations, obtaining finally a system that determines the solution vectors,

$$\Psi_{d+1/2} \equiv (J_{d+1/2,1}, \dots, J_{d+1/2,K}, T_{d+1/2}, N_{d+1/2}, n_{1,d+1/2}, \dots, n_{L,d+1/2}, n_{e,d+1/2}) \quad (2.63)$$

for $d = 1, \dots, D$. As in the LTE case, the linearized system is of the form of Eq. (2.54); the computational effort scales as $cD(N + L + 3)^3$, which, for realistic problems, becomes costly.

The direct Rybicki algorithm is unsuited to this problem because we wish to determine *several* variables at each depth point (a minimum set would be T and all level populations) so the final system to be solved becomes very large. Nevertheless efficient iterative solutions of the system may be feasible, using astute preconditioning techniques such as those being developed by Scharmer and his colleagues [47, 48]; this is a question for future research.

To obtain a non-LTE model with line transitions it has been customary to construct a sequence of models: first in LTE (which gives the asymptotic solution at great depth); next for non-LTE continua only (which accounts for departures from LTE in the most transparent transitions, hence deepest layers); finally with non-LTE in the full transition array. Details are discussed in [35]. Little is known about the necessity and/or efficacy of this cautious ritual.

Very little effort has been devoted to finding cheaper methods. Anderson [1] has

suggested a very promising approach which uses heuristic arguments to prescribe groupings of large numbers of individual frequencies into coarse bins which are treated internally by a kind of multifrequency/grey method. To the author's knowledge no attempts have been made to find numerical splittings of the equations like those described in [8]; such an effort might possibly prove rewarding, though past experience is not encouraging.

III. SPHERICAL GEOMETRY

Many astrophysical media can be considered spherical (e.g., stars) or spherical shells (e.g., planetary nebulae).

A. The Transfer Equation

In a static spherical medium the transfer equation is

$$\mu(\partial I_{\mu\nu}/\partial r) + r^{-1}(1 - \mu^2)(\partial I_{\mu\nu}/\partial \mu) = \chi_\nu(S_\nu - I_{\mu\nu}). \quad (3.1)$$

Taking symmetric and antisymmetric averages for $\pm\mu$ (and making the same assumption about the isotropy of material properties as in Sect. II) we find

$$\mu(\partial h_{\mu\nu}/\partial r) + r^{-1}(1 - \mu^2)(\partial h_{\mu\nu}/\partial \mu) = \chi_\nu(S_\nu - j_{\mu\nu}) \quad (3.2)$$

and

$$\mu(\partial j_{\mu\nu}/\partial r) + r^{-1}(1 - \mu^2)(\partial j_{\mu\nu}/\partial \mu) = -\chi_\nu h_{\mu\nu}, \quad (3.3)$$

which can be rewritten in a more conservative form as

$$\frac{\mu}{r^2} \frac{\partial}{\partial r} (r^2 h_{\mu\nu}) + \frac{1}{r} \frac{\partial}{\partial \mu} [(1 - \mu^2) h_{\mu\nu}] = \chi_\nu (S_\nu - j_{\mu\nu}) \quad (3.4)$$

and

$$\mu^2 \frac{\partial j_{\mu\nu}}{\partial r} + \frac{(3\mu^2 - 1)}{r} j_{\mu\nu} + \frac{1}{r} \frac{\partial}{\partial \mu} [\mu(1 - \mu^2) j_{\mu\nu}] = -\chi_\nu \mu h_{\mu\nu}. \quad (3.5)$$

B. Formal Solution

Suppose we are to calculate the angle-frequency dependent radiation field for a given run of $S_\nu(r)$. Discretize the medium with a set of spherical shells $\{r_d\}$ ($d = 1, \dots, D + 1$) with $r_1 = r_c$, an inner *core radius*, and $r_{D+1} = R$ the total radius of the medium; see Fig. 2. Locate $j_{\mu\nu}$ at cell centers $r_{d+1/2}$ and $h_{\mu\nu}$ on the radial shells; one can define $r_{d+1/2}$ as, for example, containing half the volume between r_d and r_{d+1} ,

$$r_{d+1/2}^3 \equiv \frac{1}{2}(r_d^3 + r_{d+1}^3). \quad (3.6)$$

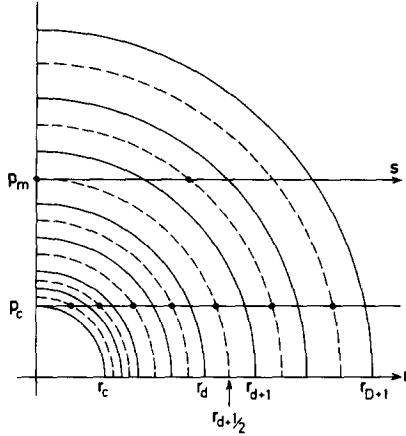


FIGURE 2

We may then proceed in one of two ways:

(i) Tangent rays. The differential operator $\mu(\partial/\partial r) + r^{-1}(1 - \mu^2)(\partial/\partial \mu)$ is identically equal to $(\partial/\partial s)$, where s measures pathlength along a ray trajectory. A particularly useful choice is a set of parallel rays tangent to the spherical shells $\{r_{d+1/2}\}$ through the cell centers. Each ray is then specified by its impact parameter p , the distance from the center along a symmetry axis perpendicular to the ray bundle; positions on a ray are specified by s , the pathlength from the symmetry axis (see Fig. 2).

Let $I_{\mu\nu}^{\pm}$ denote the intensity traveling along $\pm s$. Equation (3.1) is then

$$\pm (\partial I_{\mu\nu}^{\pm} / \partial s) = \chi(r, \nu) [S(r, \nu) - I_{\mu\nu}^{\pm}], \tag{3.7}$$

where $r = r(s, p) = (s^2 + p^2)^{1/2}$. Introducing Feautrier variables along this ray, we can rewrite Eq. (3.7) as

$$(\partial h_{sv} / \partial \tau_{sv}) = j_{sv} - S_{sv} \tag{3.8}$$

and

$$(\partial j_{sv} / \partial \tau_{sv}) = -h_{sv}, \tag{3.9}$$

which combine to yield

$$(\partial^2 j_{sv} / \partial \tau_{sv}^2) = j_{sv} - S_{sv}, \tag{3.10}$$

where $d\tau_{sv} \equiv -\chi_{\nu} ds$ and we suppressed mention to p (which is fixed). Equation (3.10) along with boundary conditions obtained from Eqs. (3.8) and (3.9) can be discretized as a tridiagonal system along the ray, and solved as in Eq. (2.38). As was true in

planar geometry, one may use second-order accurate finite differences, spline collocation, or a Hermite scheme. Details are discussed in [18, 38] and Chap. 7 of [31].

To obtain the run of $j_{\mu\nu}$ on the full range of μ one must supplement the tangent rays through cell centers by additional rays that sample the core ($p \leq p_c = r_c$). By symmetry one need solve only to the right of the vertical axis in Fig. 2. If D shells are sampled completely, the total computing effort scales as cD^2N (D is assumed to be much larger than the number of core rays). Because each ray contains a different number of nodes, the algorithm does not vectorize over p , but can be vectorized over frequency on each ray.

An advantage of the tangent ray method is that it can handle the sharp forward peaking of the radiation field that occurs in the outer regions of very extended transparent media [19].

(ii) Discrete angle-differencing. A significant drawback of the tangent-ray method is that it can never be made exactly consistent with the moment equations discussed in Section IIIc. For example, simple geometry shows that if the flux-like quantity $h_{\mu\nu}$ is to be located at $\{r_d\}$, it will be miscentered with respect to $j_{\mu\nu}$, located on a set of ray-induced nodes $\{s_{d+1/2}(p)\}$, by different amounts for each shell on a given ray and by different amounts for each ray intersecting a specified shell. Nor are the equations in any sense conservative; there is no way they can be summed to yield

Carlson's S_N -method for neutron transport [11, 26, 27].

Thus choose a set of discrete ordinates $\{\mu_m\}$, $m = 1, \dots, M$, and let j_m and h_m represent $j(\mu)$ and $h(\mu)$ within an angular cell $(\mu_{m-1/2}, \mu_{m+1/2})$. Clearly $\mu_{1/2} \equiv 0$ and $\mu_{M+1/2} \equiv 1$; the remaining cell boundaries will be prescribed shortly. Then integrating Eqs. (3.4) and (3.5) over an angle cell we obtain

$$\frac{b_m \mu_m}{r^2} \frac{\partial}{\partial r} (r^2 h_m) + \frac{1}{r} [(1 - \mu_{m+1/2}^2) h_{m+1/2} - (1 - \mu_{m-1/2}^2) h_{m-1/2}] = \chi b_m (S - j_m) \quad (3.11)$$

and

$$b_m \mu_m^2 \frac{\partial j_m}{\partial r} + \frac{b_m (3\mu_m^2 - 1)}{r} j_m + \frac{1}{r} [\mu_{m+1/2} (1 - \mu_{m+1/2}^2) j_{m+1/2} - \mu_{m-1/2} (1 - \mu_{m-1/2}^2) j_{m-1/2}] = -\chi b_m \mu_m h_m, \quad (3.12)$$

where for brevity we omit reference to frequency. Noting that $h_{1/2} = h(\mu = 0) \equiv 0$ by symmetry, we instantly see that Eqs. (3.11) and (3.12) will sum exactly to discrete representations of the moment equations (3.25) and (3.26).

An important limit that must be guaranteed by Eqs. (3.11) and (3.12) is that in an

infinite homogeneous medium $j \equiv S$ and $h \equiv 0$. Equation (3.11) admits this limit automatically, but Eq. (3.12) does only if one chooses cell boundaries such that

$$\mu_{m+1/2}(1 - \mu_{m+1/2}^2) - \mu_{m-1/2}(1 - \mu_{m-1/2}^2) = b_m(3\mu_m^2 - 1). \quad (3.13)$$

Equation (3.13) defines the $\{\mu_{m+1/2}\}$ recursively; note that it can be satisfied with even a one angle-point quadrature if we choose $\mu_1 = 1/\sqrt{3}$.

To evaluate $j_{m\pm 1/2}$ and $h_{m\pm 1/2}$ we must choose a representation for $j(\mu)$ and $h(\mu)$. A good choice on the basis of stability considerations is a linear spline [44], i.e.,

$$j_{m+1/2} = [(\mu_{m+1} - \mu_{m+1/2})j_m + (\mu_{m+1/2} - \mu_m)j_{m+1}]/(\mu_{m+1} - \mu_m), \quad (3.14)$$

and similarly for $h_{m+1/2}$. The discrete system (3.11) and (3.12) is then tridiagonal in angle. If similar equations are formulated for $I_{\mu\nu}^\pm$ instead of $j_{\mu\nu}$ and $h_{\mu\nu}$, the fact that a photon trajectory always has a larger value of μ at the point of destruction than the point of creation argues for upstream differencing in angle [29], which permits a *sequential* solution at successive angles. The argument does not apply, however, to $j_{\mu\nu}$ and $h_{\mu\nu}$, which mix information from $\pm\mu$; hence we have no choice but to solve for all angle components simultaneously.

Spatially discretized versions of Eqs. (3.11) and (3.12) with suitable boundary conditions produce a system of the form

$$-A_d \mathbf{j}_{d+1/2} + B_d \mathbf{h}_d - C_d \mathbf{j}_{d-1/2} = D_d, \quad (d = 1, \dots, D). \quad (3.15)$$

and

$$-E_{d+1/2} \mathbf{h}_{d+1} + F_{d+1/2} \mathbf{j}_{d+1/2} - G_{d+1/2} \mathbf{h}_d = H_{d+1/2}, \quad (d = 1, \dots, D). \quad (3.16)$$

Here $\mathbf{j}_{d+1/2}$ and \mathbf{h}_d are vectors of length M containing the angular variation of $j_{\mu\nu}$ and $h_{\mu\nu}$ at specified depth points, and $A, B, C, E, F,$ and G are $(M \times M)$ tridiagonal matrices. The boundary conditions imply $A_{D+1} \equiv 0$ and $C_1 \equiv 0$. The system is solved by forward elimination, generating

$$\mathbf{K}_d = (B_d - A_d \mathbf{M}_{d+1/2})^{-1} C_d, \quad (3.17)$$

$$\mathbf{L}_d = (B_d - A_d \mathbf{M}_{d+1/2})^{-1} (D_d + A_d \mathbf{N}_{d+1/2}), \quad (3.18)$$

$$\mathbf{M}_{d-1/2} = (F_{d-1/2} - E_{d-1/2} \mathbf{K}_d)^{-1} G_{d-1/2} \quad (3.19)$$

$$\mathbf{N}_{d-1/2} = (F_{d-1/2} - E_{d-1/2} \mathbf{K}_d)^{-1} (H_{d-1/2} + E_{d-1/2} \mathbf{L}_d) \quad (3.20)$$

followed by the back-substitution

$$\mathbf{h}_d = \mathbf{K}_d \mathbf{j}_{d-1/2} + \mathbf{L}_d \quad (3.21)$$

and

$$\mathbf{j}_{d+1/2} = \mathbf{M}_{j+1/2} \mathbf{h}_d + \mathbf{N}_{d+1/2} \quad (3.22)$$

for $d = 1, \dots, D$. The computational effort scales as cDM^3N , which is advantageous when D is large and M is small, as might be true for a problem with a geometrically thin transport region (e.g., a stellar atmosphere), in which forward peaking of the radiation is not severe, surrounding a large diffusion region (e.g., a star), in which sphericity effects are important (because $r_c \ll R$) but the radiation is almost isotropic. However, in very extended transparent media, the angle mesh must be specially tailored to handle forward peaking, or the number of meshpoints becomes prohibitively large. The ray method may then be preferable.

C. Scattering Problems

Scattering problems are more complex in spherical geometry than in planar geometry because the angle cosine μ between the direction of photon propagation and local outward normal varies along the ray path.

(i) Rybicki algorithm. If the scattering term contains only a single frequency-independent integral such as $\bar{J} \equiv \int \phi_\nu J_\nu dv$ we can solve the problem using a variant of the Rybicki algorithm [38] on tangent rays. Along each ray we have a tridiagonal system of the form

$$\mathbf{T}_{ln} \mathbf{j}_{ln} = \mathbf{U}_{ln} \bar{\mathbf{J}} + \mathbf{V}_{ln} \quad (l = 1, \dots, L); \quad n = 1, \dots, N), \quad (3.23)$$

where $\bar{\mathbf{J}}$ and \mathbf{j}_{ln} contain, respectively, the radial variation of \bar{J} and $j[r(s, p_l), \nu]$ on the nodes generated by the intersections of the ray specified by p_l with the radial shells. This ray contains L nodes ranging from $r = r_{l+1} = R$ to $r = p_l$. Equation (3.23) is solved to yield $\mathbf{j}_{ln} = \mathbf{C}_{ln} \bar{\mathbf{J}} + \mathbf{D}_{ln}$. We use these expressions for all (l, n) in the definition of $\bar{\mathbf{J}}$, namely

$$\bar{\mathbf{J}}_{d+1/2} = \sum_{l,n} \mathbf{w}_{ln} \mathbf{j}_{d+1/2,ln}, \quad (3.24)$$

to develop a final system of the form $\mathbf{A} \bar{\mathbf{J}} = \mathbf{B}$, which yields $\bar{\mathbf{J}}$, hence S_ν . Details of how quadrature weights are generated and how the matrices mesh together are discussed in [38]. The total computing effort scales as cD^3N , which is favorable for large N , but inefficient for coherent scattering ($N = 1$), compared to solutions using the moment equations.

(ii) The moment equations. To reduce the dimensionality of the problem (critical for constructing model atmospheres), we integrate Eqs. (3.4) and (3.5) over angle to obtain the moment equations

$$\frac{1}{r^2} \frac{\partial(r^2 H_\nu)}{\partial r} = \chi_\nu (S_\nu - J_\nu) \quad (3.25)$$

and

$$\frac{\partial(f_\nu J_\nu)}{\partial r} + \frac{(3f_\nu - 1)J_\nu}{r} = -\chi_\nu H_\nu, \quad (3.26)$$

where f_v is the variable Eddington factor. The additional term on the left-hand side of Eq. (3.26) precludes obtaining a simple second-order equation by substituting for H_v in Eq. (3.25). But as pointed out by Auer [3] one can define a *sphericity factor* q_v by

$$\ln q_v \equiv \int_{r_c}^r \left(\frac{3f_v - 1}{f_v} \right) \frac{dr'}{r'} \quad (3.27)$$

which is known if f_v is given. We can then rewrite Eq. (3.26) as

$$\partial(f_v q_v H_v) / \partial \tau_v = q_v H_v, \quad (3.28)$$

where $d\tau_v \equiv -\chi_v dr$, and thus obtain from Eq. (3.25) the *combined moment equation*

$$\frac{1}{q_v} \frac{\partial}{\partial \tau_v} \left[\frac{r^2}{q_v} \frac{\partial(f_v q_v J_v)}{\partial \tau_v} \right] = \frac{r^2}{q_v} (J_v - S_v). \quad (3.29)$$

Defining the new independent variable $dX_v \equiv (q_v/r^2) d\tau_v$, we can rewrite Eq. (3.29) as

$$\frac{\partial^2(f_v q_v J_v)}{\partial X_v^2} = \left(\frac{r^4}{q_v} \right) (J_v - S_v). \quad (3.30)$$

Boundary conditions follow from Eqs. (3.25), (3.26), and (3.28); see [38] and Chap. 7 in [31].

(iii) Feautrier algorithm. On a discrete radius mesh Eqs. (3.30) and its boundary conditions produce a block tridiagonal system as in Eq. (2.30). Given values of f_v and q_v we solve it by the same algorithm to obtain $J_v(r)$ at all radii and frequencies with a computational effort scaling as cDN^3 , where N is the number of frequency points needed to represent the scattering kernel in

$$S_v = \alpha_v \int R(v', v) J_{v'} dv' + \beta_v. \quad (3.31)$$

Clearly this scaling is most favorable for problems with large D and small N (e.g., coherent scattering, $N = 1$).

As in the planar problem, a solution of Eq. (3.30), which yields correct global thermalization, is followed by a formal solution to determine the angular variation of $j_{\mu\nu}$, hence improved Eddington and sphericity factors f_v and q_v . One iterates between the moment equations and formal solution until convergence is obtained; for I iterations the total computational effort scales as $I(cDN^3 + c'D^2N)$ or $I(cDN^3 + c'DM^3N)$ for the tangent ray and discrete space formal solutions, respectively.

A difficulty with the procedure just outlined is that it is not possible to obtain strict *consistency* between the combined moment equations and the formal solution even though tight *convergence* is obtained. The problems are: (1) There is no way of calculating q_v from a discrete set of f_v 's in such a way as to guarantee the discrete versions of Eqs. (3.26) and (3.28) are exactly consistent. The possibility of

consistency is further eroded when we introduce the new variable X_ν and base a difference scheme on Eq. (3.30). (2) The tangent rays produce a coordinate system which is obviously not orthogonal to r . Therefore summation over tangent rays to effect an angle integration cannot commute with spatial differencing in r . In contrast, if one uses Eqs. (3.11) and (3.12) for the formal solution and Eqs. (3.25) and (3.26) for the moment solution, exact consistency is achievable.

D. The Model Atmospheres Problem

When Eq. (3.30) is coupled to constraints of radiative equilibrium, hydrostatic equilibrium (generalized to spherical geometry), and either LTE or non-LTE material equations, the resulting discrete system has precisely the same mathematical structure as the planar model atmospheres problem and can be solved by the same algorithms. Details and typical applications appear in [12, 25, 37, 38].

IV. TIME-DEPENDENT TRANSPORT IN PLANAR MEDIA

For some applications it is of interest to consider time-dependent propagation of radiation in a static medium (assumed planar here). The transport equation is

$$\frac{1}{c} \frac{\partial I_{\mu\nu}^\pm}{\partial t} \pm \mu \frac{\partial I_{\mu\nu}^\pm}{\partial z} = \chi_\nu (S_\nu - I_\nu). \quad (4.1)$$

Taking symmetric and antisymmetric averages of Eq. (4.1) we get

$$\frac{1}{c} \frac{\partial j_{\mu\nu}}{\partial t} + \mu \frac{\partial h_{\mu\nu}}{\partial z} = \chi_\nu (S_\nu - j_{\mu\nu}) \quad (4.2)$$

and

$$\frac{1}{c} \frac{\partial h_{\mu\nu}}{\partial t} + \frac{\partial j_{\mu\nu}}{\partial z} = -\chi_\nu h_{\mu\nu}. \quad (4.3)$$

These equations limit to the wave equation in transparent media, the time-dependent diffusion equation in opaque media, and have the correct flux-limiting properties [39, 40, 41].

We may discretize Eqs. (4.2) and (4.3) on a staggered spatial mesh such as in Fig. 1. To handle the time derivatives several options are open: the method of lines [8], finite differences, or partial analytical integration [41]. For simplicity choose finite differences. Experience shows that the dispersiveness of time-centered schemes (e.g., Crank–Nicholson) produces unacceptable oscillations behind steep fronts, hence one opts for a diffusive scheme such as backward Euler (fully implicit) [23, 39]. We then have

$$\mu(\partial h_{\mu\nu}/\partial z) = (\chi_\nu S_\nu + \gamma j_{\mu\nu}^-) - (\chi_\nu + \gamma) j_{\mu\nu} \quad (4.4)$$

and

$$\mu(\partial j_{\mu\nu}/\partial z) = \gamma h_{\mu\nu}^- - (\chi_\nu + \gamma) h_{\mu\nu}, \quad (4.5)$$

where $\gamma \equiv 1/c\Delta t$, $j_{\mu\nu}^-$ and $h_{\mu\nu}^-$ refer to values at the old time-level, and all other quantities are at the advanced time level. We see that the time variation of the solution manifests itself as effective source-sink terms

done for the moment equations in [16]); the relative merits of these approaches are unknown, but the latter is easier to derive and code. Boundary conditions follow directly from Eqs. (4.2) and (4.3) and specification of imposed intensities (if any).

For problems where either the source function contains a frequency-independent scattering integral (e.g., coherent scattering or complete redistribution in lines) or responds to a single integral constraint (e.g., ΔT of the material is expressed in terms of a net absorption-emission integral), we can use a Rybicki-like algorithm to solve either the coupled first-order equations (4.4) and (4.5) or their second-order counterpart. In either case the system has the form

$$\mathbf{T}_k \mathbf{X}_k = \mathbf{U}_k \bar{\mathbf{J}} + \mathbf{V}_k, \quad (4.6)$$

where k specifies a choice (μ_k, ν_k), $\bar{\mathbf{J}}$ is the depth variation of the effective scattering integral, \mathbf{V}_k contains sources (thermal and terms from old time level), and \mathbf{T}_k is tridiagonal. For the coupled first-order systems \mathbf{X}_k contains an interleaving of \mathbf{j}_k and \mathbf{h}_k ; for the second-order system only \mathbf{j}_k is needed. As before, Eq. (4.6) is solved for $\mathbf{X}_k = \mathbf{A}_k \bar{\mathbf{J}} + \mathbf{B}_k$, and this expression is summed into the discrete representation of $\bar{\mathbf{J}}$ to develop a final system for $\bar{\mathbf{J}}$. Solving for $\bar{\mathbf{J}}$ we can evaluate S_ν , hence construct $\mathbf{j}_{\mu\nu}$ from systems of the form of Eq. (2.28). The total computing effort scales as $cD^2K + c'D^3$.

If the scattering integral is explicitly frequency dependent, or we wish to satisfy several constraints (e.g., energy balance plus non-LTE rate equations), a Feautrier scheme based on moment equations is more appealing. One integrates Eqs. (4.2) and (4.3) over angle and introduces Eddington factors. One solves these equations for J_ν , hence can evaluate S_ν , and then updates the Eddington factors from a formal solution, iterating the whole process to convergence. While approach has, in fact, worked in some dynamical calculations on *fluid-flow* timescales (so the radiation is essentially quasi-static), its efficacy in general is unknown. In particular for the propagation of steep radiation fronts on *radiation-flow* timescales there may be unsatisfactory feedback between the two steps of the iteration. Indeed computing radiation-front propagation accurately remains troublesome. One wants better resolution than given by the diffusive backward Euler scheme, while avoiding spurious ringing. Perhaps techniques developed in other contexts—flux-corrected transport (FCT), monotonized advection, adaptive meshes—could be helpful here. Little work has yet been done, and this area is ripe for systematic study.

ACKNOWLEDGMENTS

It is a great pleasure to thank Professor Dr. R. Kippenhahn for the gracious hospitality he has offered me during my visit to his institute, and the Alexander von Humboldt Stiftung for the award that made that visit possible. I am delighted to thank Dr. Karl-Heinz Winkler for intense scientific stimulation, many penetrating discussions, and encouragement and inspiration. I also offer my warm thanks to my good friends Lawrence Auer, Paul Kunasz, and David Hummer in remembrance of the insights we shared; the hard work we did together in developing some of the methodology described herein and in struggling to understand its strengths and weaknesses; and for the good times we had doing it. Finally I thank Berni Alder for suggesting that I write this article and for reminding me to keep my promise to do it!

REFERENCES

1. L. S. ANDERSON, *Bull. Am. Astron. Soc.* **14** (1982), 921.
2. L. H. AUER, *Astrophys. J. Lett.* **150** (1967), L53.
3. L. H. AUER, *J. Quant. Spectrosc. Radiat. Transfer* **11** (1971), 573.
4. L. H. AUER, *J. Quant. Spectrosc. Radiat. Transfer* **16** (1976), 931.
5. L. H. AUER AND D. MIHALAS, *Astrophys. J.* **158** (1969), 641.
6. L. H. AUER AND D. MIHALAS, *Mon. Not. Roy. Astron. Soc.* **149** (1970), 60.
7. L. H. AUER AND D. MIHALAS, *Astrophys. J. Suppl.* **24** (1972), 193.
8. T. S. AXELROD, P. F. DUBOIS, AND C. E. RHOADES, JR., *J. Comput. Phys.* **54** (1984), 205.
9. C. J. CANNON, *Astrophys. J.* **161** (1970), 255.
10. C. J. CANNON AND D. E. REES, *Astrophys. J.* **169** (1971), 157.
11. B. G. CARLSON, *Methods Comput. Phys.* **1** (1963), 1.
12. J. I. CASTOR, *Astrophys. J.* **189** (1974), 273.
13. P. FEAUTRIER, *C. R. Acad. Sci. Paris* **258** (1964), 3189.
14. P. FEAUTRIER, *Ann. Astrophys.* **30** (1967), 125.
15. P. FEAUTRIER, *Ann. Astrophys.* **31** (1968), 257.
16. B. E. FREEMAN, L. E. HAUSER, J. T. PALMER, S. O. PICKARD, G. M. SIMMONS, D. G. WILLISTON, AND J. E. ZERKLE, "The VERA Code: A One-Dimensional Radiative Hydrodynamic Program, Vol. I," DASA Report No. 2135, Systems, Science, and Software, Inc., La Jolla, Calif., 1968.
17. B. GUSTAFSSON AND P. NISSEN, *Astron. Astrophys.* **19** (1972), 261.
18. D. G. HUMMER, C. V. KUNASZ, AND P. B. KUNASZ, *Comput. Phys. Commun.* **6** (1973), 38.
19. D. G. HUMMER AND G. B. RYBICKI, *Mon. Not. R. Astron. Soc.* **152** (1971), 1.
20. T. L. JORDAN, "Program Library Write-Up F463, TRIDEC and TRISLV," Los Alamos Nat. Laboratory, Los Alamos, N. Mex., 1979.
21. T. L. JORDAN, "Program Library Write-Up F430, SGEFA," Los Alamos Natl. Laboratory, Los Alamos, N. Mex., 1979.
22. T. L. JORDAN, "SGESLM: Solution of Linear System with Multiple Right-Hand Sides," private communication, 1983.
23. P. B. KUNASZ, *Astrophys. J.* **271** (1983), 321.
24. P. B. KUNASZ AND D. G. HUMMER, *Mon. Not. R. Astron. Soc.* **166** (1974), 19.
25. P. B. KUNASZ, D. G. HUMMER, AND D. MIHALAS, *Astrophys. J.* **202** (1975), 92.
26. K. D. LATHROP AND B. G. CARLSON, *J. Comput. Phys.* **2** (1967), 173.
27. K. D. LATHROP AND B. G. CARLSON, *J. Quant. Spectrosc. Radiat. Transfer* **11** (1971), 921.
28. L. LUCY, in "Proceedings of the First Harvard-Smithsonian Conference on Stellar Atmospheres," Smithsonian Astrophysical Observatory Special Report No. 167, Cambridge, Mass., 1964.
29. C. M. LUND AND J. R. WILSON, Lawrence Livermore Laboratory Report No. UCRL-84678, Livermore, Calif., 1980.
30. D. MIHALAS, *Astrophys. J.* **176** (1972), 139.

31. D. MIHALAS, "Stellar Atmospheres," 2nd ed., Freeman, San Francisco, 1978.
32. D. MIHALAS, *Astrophys. J.* **237** (1980), 574.
33. D. MIHALAS, *J. Quant. Spectrosc. Radiat. Transfer* **25** (1981), 145.
34. D. MIHALAS AND L. H. AUER, *Astrophys. J.* **160** (1970), 1161.
35. D. MIHALAS, L. H. AUER, AND J. N. HEASLEY, NCAR Technical Note No. TN/STR-104, National Center for Atmospheric Research, Boulder, Colo., 1975.
36. D. MIHALAS, L. H. AUER, AND B. R. MIHALAS, *Astrophys. J.* **220** (1978), 1001.
37. D. MIHALAS AND D. G. HUMMER, *Astrophys. J. Lett.* **189** (1974), L39.
38. D. MIHALAS AND D. G. HUMMER, *Astrophys. J. Suppl.* **28** (1974), 343.
39. D. MIHALAS AND R. I. KLEIN, *J. Comput. Phys.* **46** (1982), 97.
40. D. MIHALAS AND B. W. MIHALAS, "Foundations of Radiation Hydrodynamics," Oxford Univ. Press, New York, 1984.
41. D. MIHALAS AND R. P. WEAVER, *J. Quant. Spectrosc. Radiat. Transfer* **28** (1982), 213.
42. D. MIHALAS, K.-H. A. WINKLER, AND M. L. NORMAN, *J. Quant. Spectrosc. Radiat. Transfer* **31** (1984), 479.
43. R. W. MILKEY, R. A. SHINE, AND D. MIHALAS, *Astrophys. J.* **202** (1975), 250.
44. A. PERAIAH AND I. P. GRANT, *J. Inst. Maths. Appl.* **12** (1973), 75.
45. G. C. POMRANING, "Equations of Radiation Hydrodynamics," Pergamon, Oxford, 1973.
46. G. B. RYBICKI, *J. Quant. Spectrosc. Radiat. Transfer* **11** (1971), 589.
47. G. B. SCHARMER, *Astrophys. J.* **249** (1981), 720.
48. G. B. SCHARMER AND M. CARLSSON, *J. Comput. Phys.*, in press.
49. R. N. THOMAS, "Some Aspects of Non-Equilibrium Thermodynamics in the Presence of a Radiation Field," Univ. of Colorado Press, Boulder, Colo., 1965.
50. B. E. WOLF, F. SCHMITZ, AND P. ULMSCHNEIDER, *Astron. Astrophys.* **97** (1981), 101.